

2018

## Estimating taxon-specific population dynamics in diverse microbial communities

Benjamin J. Koch  
*Northern Arizona University*

Theresa A. McHugh  
*Northern Arizona University & Colorado Mesa University*

Michaela Hayer  
*Northern Arizona University*

Egbert Schwartz  
*Northern Arizona University*

Steven J. Blazewicz  
*Lawrence Livermore National Laboratory*

*See next page for additional authors*

Follow this and additional works at: [https://researchrepository.wvu.edu/faculty\\_publications](https://researchrepository.wvu.edu/faculty_publications)



Part of the [Plant Sciences Commons](#)

---

### Digital Commons Citation

Koch, Benjamin J.; McHugh, Theresa A.; Hayer, Michaela; Schwartz, Egbert; Blazewicz, Steven J.; Dijkstra, Paul; Gestel, Natasja Van; Marks, Jane C.; Mau, Rebecca L.; Morrissey, Ember M.; Pett-Ridge, Jennifer; and Hungate, Bruce A., "Estimating taxon-specific population dynamics in diverse microbial communities" (2018). *Faculty & Staff Scholarship*. 2095.  
[https://researchrepository.wvu.edu/faculty\\_publications/2095](https://researchrepository.wvu.edu/faculty_publications/2095)


This Article is brought to you for free and open access by The Research Repository @ WVU. It has been accepted for inclusion in Faculty & Staff Scholarship by an authorized administrator of The Research Repository @ WVU. For more information, please contact [ian.harmon@mail.wvu.edu](mailto:ian.harmon@mail.wvu.edu).

---

## Authors

Benjamin J. Koch, Theresa A. McHugh, Michaela Hayer, Egbert Schwartz, Steven J. Blazewicz, Paul Dijkstra, Natasja Van Gestel, Jane C. Marks, Rebecca L. Mau, Ember M. Morrissey, Jennifer Pett-Ridge, and Bruce A. Hungate

## Estimating taxon-specific population dynamics in diverse microbial communities

BENJAMIN J. KOCH,<sup>1,†</sup> THERESA A. MCHUGH,<sup>1,5</sup> MICHAELA HAYER,<sup>1</sup> EGBERT SCHWARTZ,<sup>1,2</sup>  
STEVEN J. BLAZEWCZ,<sup>3</sup> PAUL DIJKSTRA,<sup>1,2</sup> NATASJA VAN GESTEL,<sup>1,6</sup> JANE C. MARKS,<sup>1,2</sup> REBECCA L. MAU,<sup>1</sup>  
EMBER M. MORRISSEY,<sup>4</sup> JENNIFER PETT-RIDGE,<sup>3</sup> AND BRUCE A. HUNGATE <sup>1,2</sup>

<sup>1</sup>Center for Ecosystem Science and Society, Northern Arizona University, Flagstaff, Arizona 86011 USA

<sup>2</sup>Department of Biological Sciences, Northern Arizona University, Flagstaff, Arizona 86011 USA

<sup>3</sup>Physical and Life Sciences Directorate, Lawrence Livermore National Laboratory, Livermore, California 94550 USA

<sup>4</sup>Division of Plant and Soil Sciences, West Virginia University, Morgantown, West Virginia 26506 USA

**Citation:** Koch, B. J., T. A. McHugh, M. Hayer, E. Schwartz, S. J. Blazewicz, P. Dijkstra, N. van Gestel, J. C. Marks, R. L. Mau, E. M. Morrissey, J. Pett-Ridge, and B. A. Hungate. 2018. Estimating taxon-specific population dynamics in diverse microbial communities. *Ecosphere* 9(1):e02090. 10.1002/ecs2.2090

**Abstract.** Understanding how population-level dynamics contribute to ecosystem-level processes is a primary focus of ecological research and has led to important breakthroughs in the ecology of macroscopic organisms. However, the inability to measure population-specific rates, such as growth, for microbial taxa within natural assemblages has limited ecologists' understanding of how microbial populations interact to regulate ecosystem processes. Here, we use isotope incorporation within DNA molecules to model taxon-specific population growth in the presence of <sup>18</sup>O-labeled water. By applying this model to phylogenetic marker sequencing data collected from stable-isotope probing studies, we estimate rates of growth, mortality, and turnover for individual microbial populations within soil assemblages. When summed across the entire bacterial community, our taxon-specific estimates are within the range of other whole-assemblage measurements of bacterial turnover. Because it can be applied to environmental samples, the approach we present is broadly applicable to measuring population growth, mortality, and associated biogeochemical process rates of microbial taxa for a wide range of ecosystems and can help reveal how individual microbial populations drive biogeochemical fluxes.

**Key words:** population growth rate; population mortality rate; quantitative stable-isotope probing (qSIP); rewetting; soil bacteria; turnover.

**Received** 27 November 2017; **accepted** 4 December 2017. Corresponding Editor: Debra P. C. Peters.

**Copyright:** © 2018 Koch et al. This is an open access article under the terms of the Creative Commons Attribution License, which permits use, distribution and reproduction in any medium, provided the original work is properly cited.

<sup>5</sup> Present address: Department of Biological Sciences, Colorado Mesa University, Grand Junction, Colorado 81501 USA.

<sup>6</sup> Present address: Climate Science Center, Texas Tech University, Lubbock, Texas 79409 USA.

† **E-mail:** ben.koch@nau.edu

### INTRODUCTION

Ecological theory is built upon observations of organisms and their interactions with the biotic and abiotic environment; quantifying the dynamics of species has advanced our understanding of how ecosystems work (Huffaker 1958, Paine 1966, Connell 1978, Carpenter et al. 1987, Vitousek and Walker 1989, Strayer et al. 1999). For example,

ecologists have used population growth rates of individual species to predict outcomes of competition (Tilman 1977), trajectories of succession (Chapin et al. 1994), cycling of nutrients (Elser et al. 1996), and probabilities of local and global extinction (Morris and Doak 2002). Furthermore, population growth and mortality rates of individual species ultimately drive ecosystem processes such as primary production (Caraco et al. 1997),

decomposition (Allison and Vitousek 2004), and nutrient transformation (Lovett et al. 2006). However, the synthesis of population and ecosystem ecology in recent decades has predominantly focused on macroscopic organisms (e.g., plants and animals) and has largely ignored the population biology of microbes. Although it is widely accepted that microbes are dominant drivers of energy and material fluxes in ecosystems, relatively little is known about how their species-specific dynamics shape those fluxes.

A major limitation in linking the dynamics of individual microbial taxa to ecosystem-level processes in natural settings is the paucity of tools for identifying and observing individual microbial populations in intact ecosystems. The advent of high-throughput amplicon sequencing has enabled microbial ecologists to begin cataloging an extraordinary diversity of bacterial, archaeal, and fungal taxa in a wide range of ecosystems (Chu et al. 2010, Caporaso et al. 2011, Harris et al. 2013, Maestre et al. 2015). This advance has sparked a new era for microbial ecology by enabling powerful tests and refinements of ecological concepts originally derived from data on macroscopic organisms (Prosser et al. 2007). However, microbial ecologists still lack the basic ability to resolve population-level vital rates of individual taxa in natural and engineered environments.

Existing approaches for measuring microbial population growth have a number of shortcomings that limit their utility for integrating population- and ecosystem-level processes. Microbial growth is traditionally measured in pure culture for individual populations or at the community level in situ by counting cells or tracing the fate of isotopically labeled substrates. Although culture-based methods can yield estimates of taxon-specific growth rates under laboratory conditions, they lack the realism and complexity of most ecosystems, and the growth rates measured in such studies are unlikely to apply to natural populations. In addition, most bacteria and archaea have never been cultured (Pham and Kim 2012, Stewart 2012). Radiolabeled leucine or thymidine tracers can provide an index of bacterial growth in aggregate (Ducklow et al. 2000, Rousk and Bååth 2011), but cannot differentiate growth rates of co-occurring taxa. Similarly,  $^{14}\text{C}$  incorporation into ergosterol is used for measuring fungal-specific production (Newell and

Fallon 1991, Weyers and Suberkropp 1996), but is incapable of finer taxonomic resolution.

Other recent techniques show greater promise in estimating taxon-specific growth rates of microbes in complex assemblages. Korem et al. (2015) used coverage patterns of metagenomic sequencing reads to derive indices of growth for several human commensals and pathogens. While this approach could be applied to non-clinical settings, it is limited to fully sequenced bacterial strains with single circular chromosomes and therefore excludes the vast majority of microbial diversity. This technique was recently extended to taxa for which draft-quality genomes can be constructed via genome-resolved metagenomics (Brown et al. 2016). Nonetheless, this method is applicable only to true metagenomic data, and not to amplicon data.

Another possible means to measure taxon-specific growth rates is stable-isotope probing (SIP)—a technique that uses isotopically enriched water or organic substrates and density gradient centrifugation of extracted DNA to separate actively growing microbial taxa from inactive taxa (Radajewski et al. 2000, Schwartz 2007, Coyotzi et al. 2016). Stable-isotope probing applications typically yield categorical indices of growth and may have a bias against detecting activity in microbes with low guanine and cytosine (GC) content (Schwartz et al. 2016). However, a recent improvement to the SIP method, termed quantitative stable-isotope probing (qSIP), uses sequencing and a model of isotope incorporation into DNA to estimate isotopic enrichment for all bacterial and archaeal taxa within natural or engineered assemblages (Hungate et al. 2015). Quantitatively assessing microbial activity with this technique has already expanded our ability to answer important ecological questions. For instance, Morrissey et al. (2016) used qSIP to demonstrate how evolutionary history influences bacterial activity and carbon assimilation.

Here, we extend the qSIP approach toward the integration of population- and ecosystem-level processes by calculating taxon-specific population growth and mortality rates ( $\text{d}^{-1}$ ) for all detectable bacterial and archaeal taxa following rewetting of a seasonally dried semiarid grassland soil. We then combine those growth and mortality rates with measurements of taxon-specific abundance to derive an estimate of assemblage-wide prokaryotic

turnover that is directly comparable to those determined by bulk radiolabeling experiments, isotope dilution studies, and other techniques. By estimating taxon-specific rates of microbial growth and turnover, we highlight the potential for linking population dynamics of microbial taxa to ecosystem-level processes within highly diverse natural or engineered assemblages.

## METHODS

### Overview

To illustrate how qSIP can be applied to a microbial assemblage to estimate growth rates for individual bacterial and archaeal taxa, we used semiarid grassland soils subjected to a rewetting event after a seasonal drought (McHugh et al. 2014). Such rewetting of dry soils is a widespread phenomenon in arid and semiarid ecosystems worldwide, where seasonal rain events provide a substantial portion of annual precipitation and influence the productivity of macro- and microorganisms. Our approach consisted of incubating soils with  $^{18}\text{O}$ -labeled water and using density gradient centrifugation of extracted DNA, followed by quantitative PCR (qPCR) and sequencing of the 16S rRNA gene in the resulting density fractions to estimate—for each bacterial taxon—the magnitude of density shift resulting from incorporation of  $^{18}\text{O}$  into DNA of newly formed cells. Using additional measurements of 16S rRNA gene abundance at the beginning of the incubation, we fit a model of bacterial growth and estimated parameters describing population growth, mortality, and turnover rates for all taxa present throughout the incubation.

### Soil collection, incubation, and DNA extraction

On 2 July 2013, during the dry season preceding monsoon rains, soil was collected from a semiarid grassland located on the C. Hart Merriam Elevation Gradient in northern Arizona (35.57° N, 111.57° W; Blankinship et al. 2010, McHugh et al. 2014). Five replicate soil cores (5 cm depth and diameter) were taken at random from bare soil between plant patches. Soils were sieved (2 mm mesh) and subsampled to determine gravimetric water content (105°C). Amounts of 1 g were added to 15-mL Falcon tubes, along with either 200  $\mu\text{L}$  of water at natural abundance  $\delta^{18}\text{O}$  (referred to below as the  $^{16}\text{O}$  treatment) or  $^{18}\text{O}$ -enriched water (atom

fraction 97%). Time 0 samples ( $n = 5$ ) received no additional water and were immediately frozen at  $-40^\circ\text{C}$  until further processing. Samples with added water ( $n = 10$  in total) were incubated in the dark for 10 d and then stored at  $-40^\circ\text{C}$  until further processing.

Total genomic DNA was extracted from 0.5 g of soil in each sample using PowerLyzer PowerSoil DNA Isolation Kit according to the manufacturer's instructions, with an initial 10-min incubation at  $70^\circ\text{C}$  followed by bead beating for 90 s (MO BIO Laboratories, Carlsbad, California, USA). DNA was quantified with a Qubit Fluorometer (Life Technologies, Carlsbad, California, USA).

### CsCl density gradient centrifugation and fractionation

To separate DNA by density, 1  $\mu\text{g}$  of DNA from each sample was added to approximately 2.6 mL of a saturated CsCl and gradient buffer (200 mmol/L Tris, 200 mmol/L KCl, 2 mmol/L EDTA) solution in a 3.3-mL OptiSeal ultracentrifuge tube (Beckman Coulter, Fullerton, California, USA). The samples were spun in an Optima Max benchtop ultracentrifuge (Beckman Coulter) using a Beckman TLN-100 rotor at  $127,000 \times g$  for 72 h at  $18^\circ\text{C}$ . After centrifugation, each density gradient was divided into 15 fractions of 150–200  $\mu\text{L}$ . The density of each fraction was measured with a Reichert AR200 digital refractometer (Reichert Analytical Instruments, Depew, New York, USA). Fractions with density  $<1.65 \text{ g/mL}$  were excluded from analysis due to contamination with the displacement medium. DNA was then separated from the CsCl solution using isopropanol precipitation and resuspended in 50  $\mu\text{L}$  sterile deionized water.

### Quantitative PCR

We used qPCR to determine the total numbers of bacterial 16S rRNA gene copies in each density fraction and in whole-tube extracts for the time 0 samples. Standard curves were generated using 10-fold serial dilutions of 16S rRNA gene amplicons, which were prepared using soil DNA and primers 515F (5'-GTGCCAGCMGCCGCGGTAA-3') and 806R (5'-GGACTACVSGGGTATCTAAT-3'; Caporaso et al. 2012) containing Illumina sequence adaptors P5 (5'-AATGATACGGCGACCACCGA) and P7 (5'-CAAGCAGAAGACGGCATACGA) at the 5' end of each primer to prevent decreased

primer efficiency due to amplicon degradation (Dhanasekaran et al. 2010). Triplicate 10- $\mu$ L reactions included 1  $\mu$ L of template and 9  $\mu$ L of reaction mixture with 0.2 mmol/L of each primer, 0.01 U/ $\mu$ L Phusion Hot Start II Polymerase (Thermo Fisher Scientific, Waltham, Massachusetts, USA), 1 $\times$  Phusion HF buffer (Thermo Fisher Scientific), 3.0 mmol/L MgCl<sub>2</sub>, 6% glycerol, and 200  $\mu$ mol/L dNTPs. The assays were performed on an Eppendorf Mastercycler ep Realplex system (Eppendorf, Westbury, New York, USA), using a program of 95°C for 1 min followed by 44 cycles of 95°C for 30 s, 64.5°C for 30 s, and 72°C for 1 min. Bacterial gene copy numbers were calculated using a regression equation for each assay, relating the cycle threshold value to the known number of copies in the standards.

### 16S rRNA gene sequencing

High-throughput sequencing of the 16S rRNA gene was performed on individual density fractions for samples incubated with water, and on the pooled density fractions for time 0 samples. DNA extracts were quantified by PicoGreen (Molecular Probes, Eugene, Oregon, USA) fluorescence and normalized to 1 ng/ $\mu$ L before amplification. Two PCR steps were used to process the samples (Berry et al. 2011). Each sample was first amplified using primers 515F and 806R, which target the hypervariable V4 region (Bates et al. 2011). Amplification was performed in triplicate 8- $\mu$ L reactions containing 1 mmol/L of each primer, 0.02 U/ $\mu$ L Phusion Hot Start II Polymerase (Thermo Fisher Scientific), 1 $\times$  Phusion HF buffer (Thermo Fisher Scientific), 3.0 mmol/L MgCl<sub>2</sub>, 6% glycerol, and 200  $\mu$ mol/L dNTPs. PCR conditions were 95°C for 2 min, followed by 15 cycles of 95°C for 30 s, 55°C for 30 s, and 60°C for 4 min. Initial PCR products were checked on a 1% agarose gel. Triplicates were then pooled, diluted 10-fold, and used as template in the subsequent tailing reaction with region-specific primers that included the Illumina flowcell adapter sequences and a 12-nucleotide Golay barcode (15 cycles identical to initial amplification conditions). Products of the tailing reaction were purified with carboxylated Sera-Mag SpeedBeads (Sigma-Aldrich, St. Louis, Missouri, USA) at a 1:1 v/v ratio as described in Rohland and Reich (2012), and quantified by PicoGreen fluorescence. Equal quantities of the

reaction products were then pooled. Subsequently, the library was bead-purified once more (1:1 ratio) and quantified by qPCR using the Library Quantification Kit for Illumina (Kapa Biosciences, Woburn, Massachusetts, USA). The amplicon library was denatured and loaded at 11 pmol/L (including a 30% PhiX control) onto an Illumina MiSeq instrument (San Diego, California, USA) using 2  $\times$  150 paired-end read chemistry at Northern Arizona University's Environmental Genetics and Genomics Laboratory, returning 14.2 million reads passing filter. Sequence data were deposited in MG-Rast under project ID 21659.

### Sequence processing

The forward and reverse reads were stitched using fastq-join (Aronesty 2011) and demultiplexed with the software package Quantitative Insights into Microbial Ecology v1.7 (QIIME; Caporaso et al. 2010b). Sequences were quality-filtered with a Phred score cutoff value of 30 and checked for chimeras using USEARCH (Edgar 2010). Open reference operational taxonomic unit (OTU) picking was performed at 97% identity using UCLUST (Edgar 2010). The most abundant sequence for each OTU was aligned with PyNASt (Caporaso et al. 2010a) against the Greengenes v13\_5 database (DeSantis et al. 2006), and taxonomy was assigned using the Ribosomal Data Project classifier (Wang et al. 2007). We discarded any OTUs that accounted for <0.005% of the total sequences (Bokulich et al. 2013). Sequence processing resulted in 6.2 million reads clustering into 2119 OTUs that were used for subsequent analysis at the genus level (364 genera).

To ensure robust taxon-specific population growth estimates, we imposed two additional filtering criteria. First, some density fractions within replicates failed to yield adequate sequencing data; therefore, we calculated the proportion of total DNA contained in the failed fractions and excluded replicates with  $\geq 10\%$  of total DNA in the failed fractions. This step removed one of five replicates of the <sup>16</sup>O treatment and two of five replicates of the <sup>18</sup>O treatment from subsequent analyses. Second, to ensure that taxa occurred in a sufficient number of replicates to reliably calculate growth rates and uncertainty, we imposed the condition that taxa must occur in all three remaining <sup>18</sup>O replicates, in at least three of the four

remaining  $^{16}\text{O}$  replicates, and in at least three of the five initial “time 0” replicates. This final quality-filtering step removed only 0.6% of sequence reads and excluded 38 taxa at the genus level, resulting in 326 genera for which we estimated population growth and mortality.

#### Modeling taxon-specific population growth and mortality rates

To estimate taxon-specific bacterial growth and mortality rates from these data, we extended the model of  $^{18}\text{O}$  isotope substitution in DNA presented by Hungate et al. (2015) to include an exponential model of population growth. We used a mixing model of DNA molecular weight to estimate abundances of unlabeled and labeled DNA fragments containing copies of 16S rRNA genes. The full set of equations describing the model builds upon those presented in Hungate et al. (2015) and is summarized here.

For each bacterial taxon ( $i$ ), we assumed that the abundance of cells at time  $t$  was proportional to the abundance of 16S rRNA gene copies ( $N_{\text{TOTAL}i}$ , with units of 16S rRNA gene copies/g soil). We further assumed that changes in bacterial abundances followed an exponential growth model over the 10-d incubation period, with the net rate of population growth ( $r_i$ ) expressed in units of  $\text{d}^{-1}$ :

$$N_{\text{TOTAL}it} = N_{\text{TOTAL}i0} \times e^{r_i t} \quad (1)$$

We note that alternative growth models could also be used (e.g., linear, logistic). At time 0, the total abundance of 16S rRNA gene copies ( $N_{\text{TOTAL}i0}$ ) was equivalent to the abundance of unlabeled 16S rRNA gene copies at the beginning of the incubation ( $N_{\text{LIGHT}i0}$ ), but by the end of the incubation period, both unlabeled and labeled 16S rRNA gene copies may have been present such that:

$$N_{\text{TOTAL}it} = N_{\text{LIGHT}it} + N_{\text{HEAVY}it} \quad (2)$$

Taxon-specific abundances of 16S rRNA gene copies at the beginning ( $N_{\text{TOTAL}i0} = N_{\text{LIGHT}i0}$ ) and the end of the incubation ( $N_{\text{TOTAL}it}$ ) were calculated as the products of the total abundance of 16S rRNA gene copies across all taxa, determined by qPCR, and the relative abundance of 16S rRNA gene copies associated with taxon  $i$ , determined by sequencing. We used a linear

mixing model of DNA molecular weights to estimate the abundance of labeled 16S rRNA gene copies at the end of the incubation ( $N_{\text{HEAVY}it}$ ), and by difference, the abundance of unlabeled 16S rRNA gene copies at the end of the incubation ( $N_{\text{LIGHT}it}$ ):

$$N_{\text{LIGHT}it} = N_{\text{TOTAL}it} \times \left( \frac{M_{\text{HEAVY}i} - M_{\text{LAB}i}}{M_{\text{HEAVY}i} - M_{\text{LIGHT}i}} \right) \quad (3)$$

where for each taxon ( $i$ ),  $N_{\text{TOTAL}it}$  is the total (labeled + unlabeled) abundance of 16S rRNA gene copies at the end of the incubation,  $M_{\text{HEAVY}i}$  is the molecular weight of  $^{18}\text{O}$ -labeled DNA,  $M_{\text{LIGHT}i}$  is the molecular weight of unlabeled DNA, and  $M_{\text{LAB}i}$  is the average molecular weight of DNA (labeled + unlabeled) at the end of the  $^{18}\text{O}$ - $\text{H}_2\text{O}$  incubation. Following the procedure outlined by Hungate et al. (2015), we calculated the molecular weights of DNA at the end of the  $^{18}\text{O}$ - $\text{H}_2\text{O}$  incubation ( $M_{\text{LAB}i}$ ) for each taxon ( $i$ ), along with corresponding values for unlabeled ( $M_{\text{LIGHT}i}$ ) and maximally labeled DNA ( $M_{\text{HEAVYMAX}i}$ ). We also calculated excess atom fraction  $^{18}\text{O}$  values for all taxa. The theoretical maximum ( $M_{\text{HEAVYMAX}i}$ ) assumes 100% replacement of oxygen atoms in DNA by  $^{18}\text{O}$  (an increase of 12.07747 g/mol; Hungate et al. 2015). However, as oxygen in DNA is derived from both water and organic sources, we also estimated the maximum molecular weight of DNA that could result from assimilation of  $^{18}\text{O}$ -water ( $M_{\text{HEAVY}i}$ ). This enables a more accurate estimate of growth, by accounting for the proportion of oxygen atoms in newly synthesized DNA derived from the labeled environmental water ( $U$ ):

$$M_{\text{HEAVY}i} = 12.07747U + M_{\text{LIGHT}i} \quad (4)$$

$U$  was estimated via sensitivity analysis, with logical lower and upper bounds. Values of  $U$  were rejected as too low if they resulted in a value for fully labeled DNA that was less than the molecular weight of labeled DNA observed in the  $^{18}\text{O}$  treatment ( $M_{\text{HEAVY}i} < M_{\text{LAB}i}$ ), and values of  $U$  were rejected as too high if they resulted in estimates of unlabeled 16S rRNA gene copies at the end of the incubation that exceeded the measured abundance at the beginning of the incubation ( $N_{\text{LIGHT}it} > N_{\text{LIGHT}i0}$ ), a violation of the assumption that all newly formed DNA in the  $^{18}\text{O}$  treatment was isotopically labeled. For

all taxa, we tested values of  $U$  from 0.01 to 1.00 in 0.01 increments. In this way, we constrained  $U$  by finding the maximum range of possible values common to all taxa (0.54–0.66); we used the mean of this range ( $U = 0.60$ ) as the consensus value for all taxa.

The steps described above provided taxon-specific estimates of the total and unlabeled abundances of 16S rRNA gene copies at the beginning and end of the  $^{18}\text{O}$ -water incubation and enabled fitting the exponential growth model (Eq. 1) separately for unlabeled 16S rRNA gene copies per mass of soil and for total 16S rRNA gene copies per mass of soil. With the resulting parameter estimates, we decomposed the net population growth rate of bacterial cells into the component processes of reproduction ( $b_i$ ) and death ( $d_i$ ):

$$r_i = b_i + d_i \quad (5)$$

For each taxon, we assumed that unlabeled and labeled 16S rRNA gene copies were lost to cell death at the same rate during incubation with  $^{18}\text{O}$ -labeled water and that all newly formed 16S rRNA gene copies were labeled (i.e.,  $b_i = 0$  for unlabeled 16S copies). We therefore estimated the death rate ( $d_i$ ) of each taxon ( $i$ ) as:

$$d_i = \ln\left(\frac{N_{\text{LIGHT}it}}{N_{\text{LIGHT}i0}}\right) \times \frac{1}{t} \quad (6)$$

where  $N_{\text{LIGHT}it}$  is estimated by Eq. 3,  $N_{\text{LIGHT}i0}$  is measured directly as  $N_{\text{TOTAL}i0}$ , and  $t$  is the length of the incubation (10 d). By substituting Eqs. 5, 6 into Eq. 1, we estimated the rate of reproduction ( $b_i$ ) as:

$$b_i = \ln\left(\frac{N_{\text{TOTAL}it}}{N_{\text{LIGHT}it}}\right) \times \frac{1}{t} \quad (7)$$

For all calculations, we used bootstrap resampling (1000 iterations) of replicates within each treatment to propagate uncertainty, and we estimated taxon-specific 90% confidence intervals (CI) for reproduction rate, mortality, and net population growth rate. Calculations were performed in R (R Core Team 2015); computer code is publicly available at [https://bitbucket.org/QuantitativeSIP/qsip\\_repo](https://bitbucket.org/QuantitativeSIP/qsip_repo).

We used linear regression to examine relationships between growth rate parameters and abundance. To verify the accuracy of the qSIP-generated population growth estimates, we combined the mortality rates and abundances of all

taxa to estimate assemblage-level turnover and compared that value with empirical estimates from the literature of bulk bacterial assemblage turnover derived from radioactively labeled thymidine and leucine soil incubations, isotope dilution experiments, modeling studies, and direct cell counts. We calculated assemblage-level turnover as the sum over all taxa of the mortality rate multiplied by the proportional abundance at the beginning of the incubation.

## RESULTS

Our analysis yielded population growth and mortality rates for 326 bacterial and archaeal taxa distinguished at the level of genus, representing at least 22 different phyla. Nearly three-quarters (74%) of all soil taxa became enriched with  $^{18}\text{O}$ , as determined by the 90% CIs for excess atom fraction exceeding zero (Fig. 1). The CIs for excess atom fraction  $^{18}\text{O}$  overlapped zero for 26% of taxa. No taxon had negative  $^{18}\text{O}$  enrichment. This pattern of isotopic enrichment indicates that (1) the qSIP method of quantifying isotopic incorporation was sufficiently robust to avoid falsely detecting a decrease in  $^{18}\text{O}$  enrichment and (2) most taxa incorporated  $^{18}\text{O}$  atoms into newly synthesized DNA, supporting the conclusion that these taxa produced new cells during the incubation.

Although most taxa produced new cells, the assemblage-level total abundance of 16S rRNA gene copies declined by an order of magnitude over the course of the 10-d soil incubation, indicating substantial cell mortality in response to rewetting (day 0 bootstrapped median:  $3.0 \times 10^{10}$  16S rRNA gene copies/g soil, 90% CI:  $1.9 \times 10^{10}$ – $4.2 \times 10^{10}$  16S rRNA gene copies/g soil; day 10 bootstrapped median:  $4.2 \times 10^9$  16S rRNA gene copies/g soil, 90% CI:  $2.9 \times 10^9$ – $5.1 \times 10^9$  16S rRNA gene copies/g soil). Abundances of 16S rRNA gene copies were distributed lognormally among taxa by the end of the rewetting incubation (Fig. 2A).

In contrast, population growth and mortality rates followed a normal distribution across taxa, with a majority of genera (77%) showing negative rates of net population growth (Fig. 2B). An overwhelming majority of taxa (86%) had detectable mortality (i.e.,  $d_i < 0$ ; by convention, mortality is indicated by values of  $d$  below zero), while



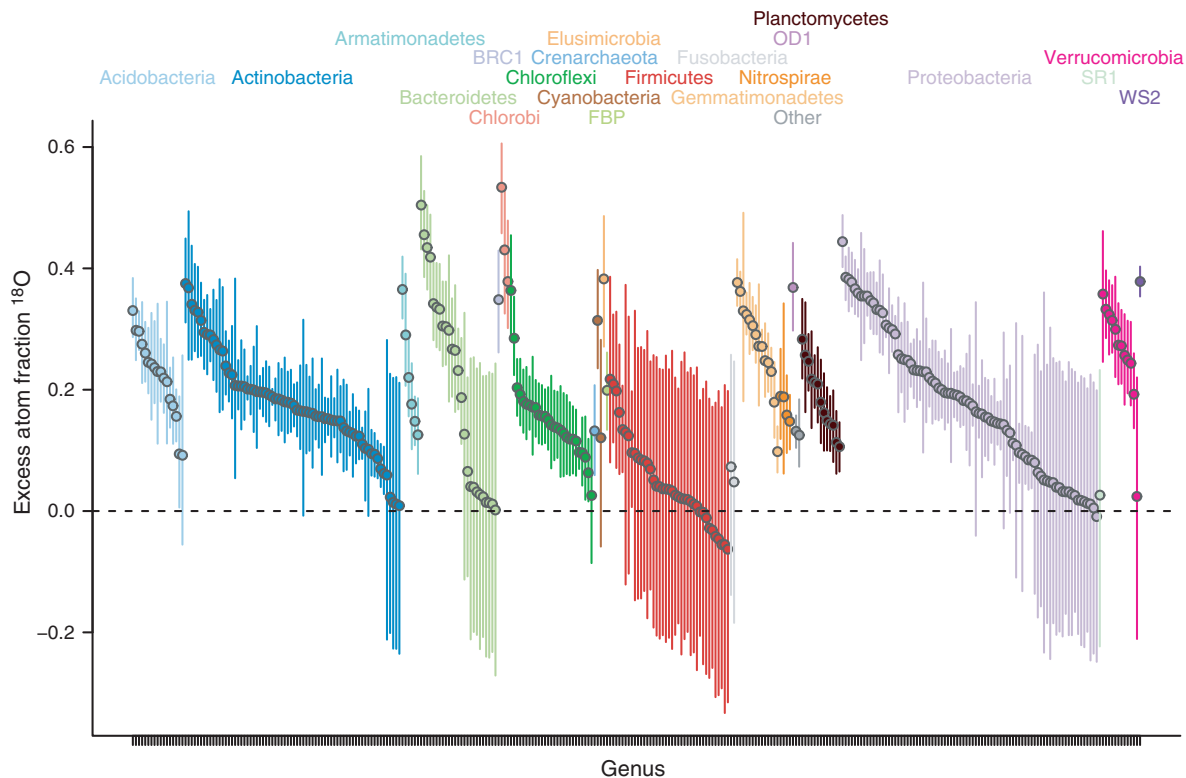


Fig. 1. A majority (74%) of the 326 prokaryotic genera present in the rewetted soil became enriched in  $^{18}\text{O}$  by the end of the 10-d incubation. The remaining 26% had excess atom fraction  $^{18}\text{O}$  values indistinguishable from zero and none had significantly negative values, indicating that the quantitative stable-isotope probing method of estimating taxon-specific isotopic enrichment was robust against detecting false deviations from zero. Points are bootstrapped medians; bars are 90% confidence intervals. Colors denote different phyla, and genera are ordered from highest enrichment to lowest enrichment within each phylum.

14% showed mortality rates indistinguishable from zero (Fig. 2B). Only one genus (*Sporocytophaga*, phylum Bacteroidetes) exhibited significant positive net population growth at the end of the incubation. Gross reproduction rates mirrored the pattern of isotopic enrichment, with 74% of taxa having positive reproduction rates and 26% of taxa showing no detectable reproduction (Fig. 2B). Together, the non-zero mortality and reproduction rates suggest that cell turnover was substantial during the incubation, with new cells produced more slowly than the rate at which they were lost to death for most bacterial populations.

Across all taxa, rates of new cell production were weakly related to the abundance of 16S rRNA gene copies at the end of the rewetting incubation and were highly variable among

genera (Fig. 3A). The positive slope suggests that taxa responding to rewetting with rapid growth became more abundant in the microbial assemblage, but the weak relationship indicates that the rate of new cell production over the 10-d period was only a partial determinant of dominance. Rates of new cell production ( $b$ ) and mortality ( $d$ ) were unrelated ( $b = 0.034 - 0.026 \times d$ ;  $n = 326$ ,  $R^2 = 0.003$ ,  $P = 0.312$ ), indicating that rapidly growing taxa did not have especially low or high rates of mortality. Mortality rates were density-dependent; abundant taxa at the beginning of the incubation experienced the greatest mortality in response to soil rewetting (Fig. 3B).

By combining the mortality rates and abundance of all 326 bacterial and archaeal genera, we calculated an assemblage-level estimate of

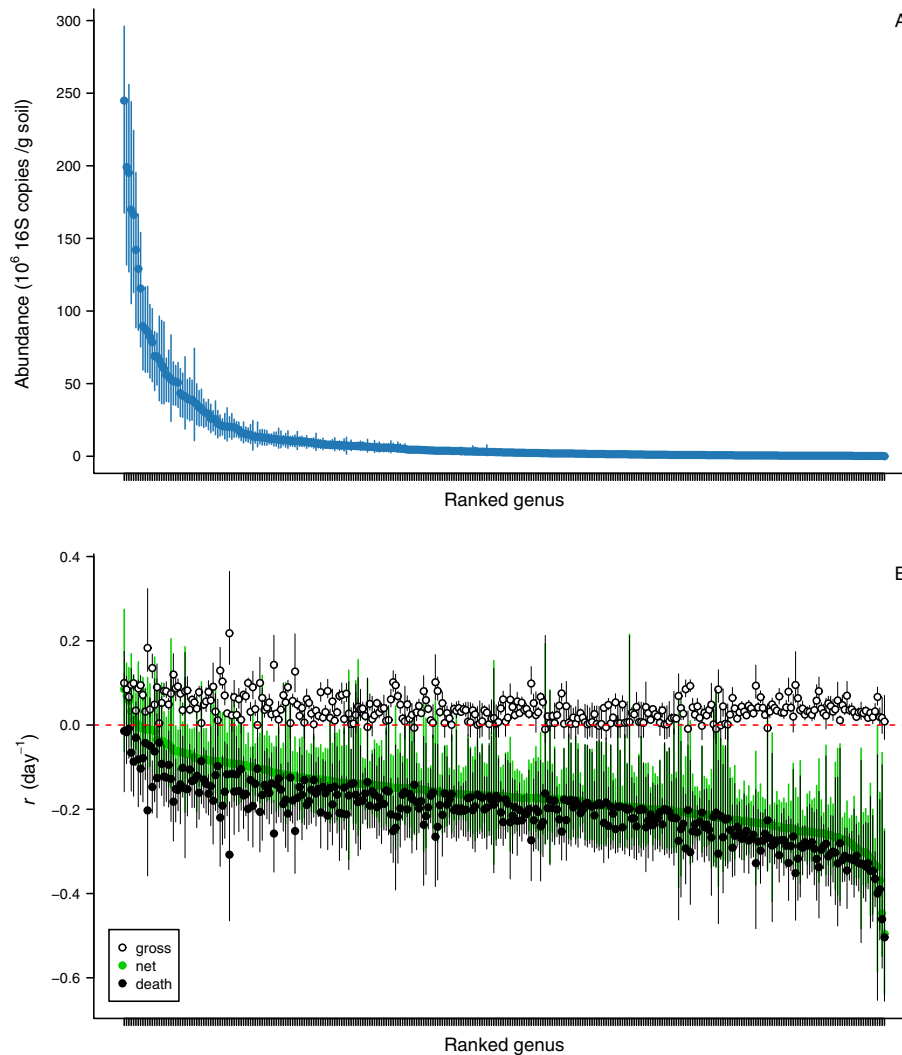


Fig. 2. (A) Taxon-specific abundances of 16S rRNA gene copies at the end of the rewetting incubation (day 10) were approximately lognormally distributed, whereas (B) population growth rates ( $r$ ) followed a normal distribution across genera. Nearly all taxa declined in abundance in response to soil rewetting (net population growth rate,  $r < 0$ ; green circles) because mortality rates ( $d$ , filled black circles) outweighed rates of reproduction ( $b$ , open circles). Points indicate bootstrapped medians; bars are 90% confidence intervals. Genera are ranked independently in each panel.

turnover that was within the range of published soil bacterial assemblage turnover rates for different ecosystems estimated from bulk radiolabeling experiments and other methods (Fig. 4). Whole-assemblage turnover estimated via qSIP using the isotope substitution and growth model presented here had an average value of  $0.287 \text{ d}^{-1}$  (90% CI:  $0.212\text{--}0.377 \text{ d}^{-1}$ ). The median estimate of soil bacterial turnover across 14 studies from the literature was  $0.197 \text{ d}^{-1}$ , with the

full range of estimates spanning  $0.003\text{--}1.14 \text{ d}^{-1}$  (Fig. 4).

## DISCUSSION

Our results show how taxon-specific population growth and mortality rates can be derived by incubating microbial communities with a stable-isotope tracer that is universally incorporated into the DNA of new cells. This technique is

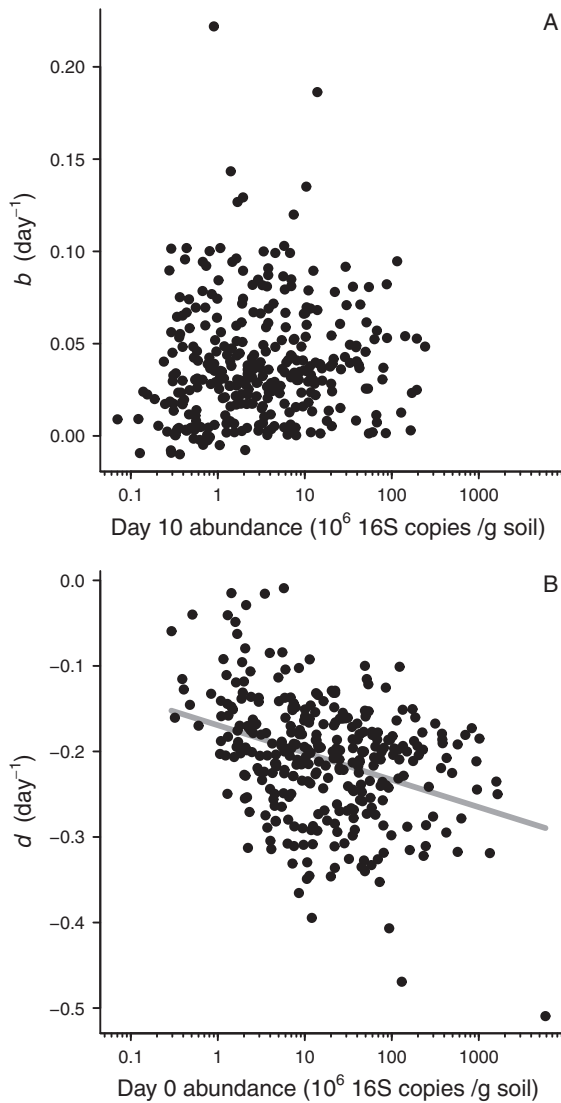


Fig. 3. (A) Rates of reproduction ( $b$ ) varied widely among prokaryotic genera and marginally increased with genus-level abundance of 16S rRNA gene copies at the end of the rewetting incubation ( $y = 0.009 + 0.005 \times \log_{10}[x]$ ;  $n = 326$ ,  $R^2 = 0.011$ ,  $P = 0.064$ ). Thus, there was a weak trend that those prokaryotic taxa that grew rapidly in response to rewetting became dominant assemblage members over time. (B) Mortality rates ( $d$ ) were greatest (more negative) for taxa with high initial abundances of 16S rRNA genes ( $y = 0.022 - 0.032 \times \log_{10}[x]$ ;  $n = 326$ ,  $R^2 = 0.121$ ,  $P < 0.0001$ ), indicating that initially dominant prokaryotes died rapidly with soil rewetting.

A generalizable to microbial assemblages in many ecosystems and distinguishes among taxa with the same resolution achieved by high-throughput amplicon sequencing. Accordingly, the qSIP approach for estimating taxon-specific microbial population dynamics complements existing tools for assessing the diversity and abundance of microbes in natural environments and enables more robust tests of ecological theory with microbial data.

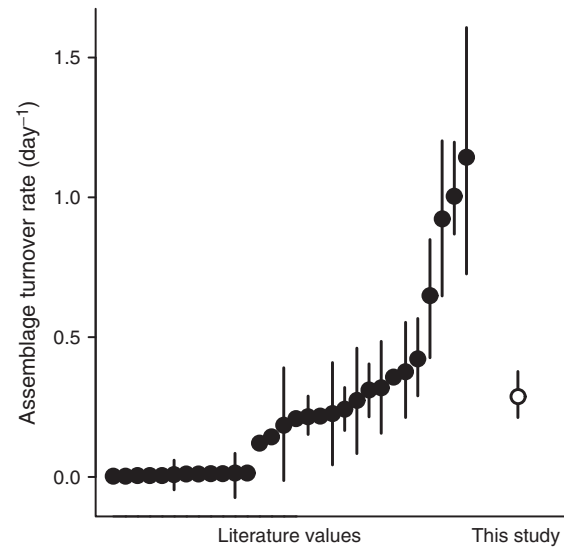


Fig. 4. The quantitative stable-isotope probing-estimated assemblage-level turnover rate of soil bacteria and archaea in this study—calculated by combining taxon-specific turnover rates across all 326 genera—is within the range of published soil bulk bacterial assemblage turnover rates measured via radiolabeled thymidine or leucine, bulk isotope dilution experiments, direct cell counts, and respiration-based modeling studies. The value from this study (open circle) is the median of 1000 bootstrap estimates; error bars indicate 90% confidence intervals (CI). Literature values (filled circles) are medians and 90% CIs corresponding to the normal distribution defined by the mean and standard deviation reported in each study. Sources of the literature values are Hunt et al. (1987), Bååth (1990, 1992), Bloem et al. (1992), Bååth (1994a, b), Harris and Paul (1994), Tibbles and Harris (1996), Bååth (1998), Kouno et al. (2002), Uhlířová and Šantrůčková (2003), Perelo and Munch (2005), Cheng (2009), and Spohn et al. (2016).

The ability to estimate taxon-specific population dynamics within microbial assemblages has important implications for ecology. Resolving population growth rates for co-occurring microbes enables more precise inferences of species interactions like competition and predation, the outcomes of which depend strongly on vital rates (Tilman 1977). For example, microbial interaction networks constructed from relative abundance data alone may not accurately reflect species interactions (Berry and Widder 2014). Incorporating additional information on growth, mortality, and turnover rates—estimated via qSIP—could enable detecting the fingerprints of species interactions. Specific interactions among organisms—mutualism, amensalism, competition, and predation—produce specific expectations about vital rates of ostensibly interacting taxa, and in this way, likely interactions can be discerned from spurious correlations. Because the qSIP approach can inform our understanding of such microbial interactions, it has the potential to vastly extend the size spectrum of organisms included in food web analyses (Schmid-Araya et al. 2002).

Measuring taxon-specific growth and mortality can also facilitate confronting existing community and ecosystem models with highly resolved population data from microbial communities. Such tests would improve our understanding of the role of microbes in ecosystems and advance ecological theory (Prosser et al. 2007). For example, by applying qSIP to derive time series of abundance, growth, and mortality, classical theories of succession (Odum 1960, Connell and Slatyer 1977, Tilman 1985) and community assembly (Post and Pimm 1983, Moyle and Light 1996, Tilman 1999) could be tested for microbial assemblages, something only rarely possible for macroscopic organisms. Furthermore, the ability to link population dynamics of individual microbial taxa to biogeochemical processes might illuminate whether a handful of hyper-abundant foundation taxa (Ellison et al. 2005) drive element fluxes, or whether they are instead regulated by rare keystone taxa (Power et al. 1996). Applications of qSIP in this vein have already revealed that microbial activity varies with phylogeny (Morrissey et al. 2016) and that the enigmatic phenomenon of priming—in which pulses of new organic matter enhance the decomposition of older organic matter—is mediated by taxa across the phylogenetic spectrum (Morrissey et al. 2017).

Estimating microbial population growth also paves the way for making taxon-specific estimates of prokaryotic production. For example, by applying to our data the simplifying assumptions that all prokaryotic taxa contain six 16S rRNA gene copies per cell (despite the known variability; Crosby and Criddle 2003, Acinas et al. 2004, Case et al. 2007) and that an average cell contains 0.1 pg carbon (C; Bölder et al. 2002), then assemblage-level prokaryotic production was  $2.76 \mu\text{g C} \cdot [\text{g soil}]^{-1} \cdot \text{d}^{-1}$  and assemblage-level loss of C to cell death was 22 times higher. The dominant taxon in terms of production comprised unidentified members of the order RB41 (phylum Acidobacteria), which was extremely abundant but grew at a relatively modest rate. Conversely, members of the order Sphingobacteriales (phylum Bacteroidetes) were not particularly abundant, but had high productivity owing to their rapid growth rates. Future applications of qSIP to estimate taxon-specific production could be improved by accounting for taxonomic variation in the number of 16S rRNA gene copies per cell, which typically range from 2 to 15 (Markowitz et al. 2012, Langille et al. 2013). However, even with that additional information, absolute abundances would still be approximate, due to the challenges of quantitatively extracting DNA from free-living cells (Martin-Laurent et al. 2001), as well as amplification and sequencing biases (Kanagawa 2003, Kozarewa et al. 2009, Tedersoo et al. 2010). The inability to measure absolute abundance and cell size of microbes remains a constraint on our ability to link taxon-specific fluxes to biogeochemical processes. Nevertheless, developing tools for even coarse estimates of taxon-specific production will advance our ability to connect biogeochemical fluxes in ecosystems with their population- and community-level drivers (Hutchinson 1942, Lindeman 1942).

A high level of phylogenetic resolution in population dynamics and element fluxes opens the door to a more intricate understanding of microbial natural history (Lazcano 2011). In the same way that detailed natural history knowledge has informed the ecology of macroscopic organisms (Tewksbury et al. 2014), uncovering the unique responses of different bacteria to environmental conditions can lead to better predictions for how ecosystems respond to environmental change.

For example, Blazewicz et al. (2014) found high bacterial and fungal mortality and population turnover following rewetting of a northern California grassland soil. Despite those changes in dynamics, population abundances remained relatively stable. Although we observed net decreases in population abundances, our data similarly suggest that such high mortality and turnover are shared by most of the bacterial taxa present in rewetted soil. Only one genus, *Sporocytophaga* (phylum Bacteroidetes), had a net positive rate of reproduction in response to rewetting. *Sporocytophaga* is adapted to dry conditions and readily forms microcysts in desiccated soils (Grace 1951, Reichenbach 2006). Our observations that this genus also had low mortality and relatively high rates of new growth following soil rewetting suggest that it may be able to take advantage of rapidly increasing soil moisture and the accompanying massive cell death of other taxa. In contrast to *Sporocytophaga*, we found that all members of the class Clostridia (phylum Firmicutes) had rates of new growth indistinguishable from zero, indicating that this group may respond more slowly to increases in soil moisture, possibly as oxygen becomes depleted.

Our estimate of aggregate bacterial assemblage turnover was within the range of those previously published, though that range is quite large, from 0.003 to 1.14 d<sup>-1</sup> (Fig. 4). Some methods of estimating bulk turnover rely on isotope tracer additions (Bååth 1990) and involve disturbing the soils, through sieving, mixing, and altering the water content. Such disturbances are known to increase microbial metabolism (Franzluebbers 1999) and may well increase estimates of turnover compared to those modeled based on microbial respiration and biomass in more intact soils (Cheng 2009). As applied here, our method also involved soil disturbance, so our aggregate estimate of turnover (0.287 d<sup>-1</sup>) may also be elevated compared to what occurs in undisturbed conditions. Additionally, the qSIP technique with <sup>18</sup>O-H<sub>2</sub>O involves adding water, so estimates may most closely approximate those following rainfall, which are likely elevated compared to dry soils (Blazewicz et al. 2014). It may be possible to minimize disturbance in future applications of qSIP, for example, by applying the <sup>18</sup>O-H<sub>2</sub>O tracer to a structurally intact soil. While the estimates presented here may not reflect field conditions, this qSIP-based

approach has the advantage of resolving rates of growth and mortality for individual taxa.

Comparing the results of the qSIP approach to other techniques also indicates that the precision of qSIP growth estimates was moderate and that nucleotide recycling during the incubation was low. The uncertainty of the qSIP growth estimates was within the range of precision of other methods for quantifying bacterial growth (Fig. 4), with the coefficient of variation in bootstrapped growth rates averaging 0.27 across all 326 taxa. Improved methods of fractionating and measuring the density of the CsCl solution after ultracentrifugation would improve the precision of qSIP-derived excess atom fraction and growth estimates. Furthermore, using qSIP to estimate growth relies on utilization of oxygen from water to synthesize new DNA, and such an approach might underestimate growth rates if nucleotide recycling occurs, if newly formed cells incorporated pre-existing, unlabeled nucleotides or recycled labeled ones. Our aggregate estimates of turnover were within the range of those previously reported based on radiolabeling experiments measuring bulk bacterial incorporation of thymidine or leucine (Bååth 1990, 1992, 1994a, b), suggesting that nucleotide recycling was low.

The qSIP approach for estimating taxon-specific population growth and mortality is generalizable to other taxa and ecosystems. Although we targeted the V4 region of the 16S rRNA gene to characterize population dynamics of bacteria and archaea, the technique could conceivably be applied to any conserved region of interest, or even to the full metagenome. For example, the internal transcribed spacer region of rRNA genes could be used to assess taxon-specific fungal growth rates, and universal mitochondrial and nuclear markers (cytochrome oxidase; 18S and 28S rRNA genes) may provide a means to estimate growth rates of other eukaryotic microorganisms. Furthermore, although our example focused on soil, the approach could be adapted to a number of other microbial communities including those associated with freshwater and marine planktonic and sediment environments, plant and animal microbiomes, and assemblages of decomposers. One constraint of the method is that it requires the addition of water, which may limit its applicability under certain environmental conditions. However, we note that qSIP has also been successfully applied to freshwater microbial

assemblages associated with decomposing leaves by replacing a portion of environmental water with  $^{18}\text{O}$ -labeled water (Hayer et al. 2016).

Knowledge of the rate processes of individual populations of macroscopic organisms within diverse species assemblages has strengthened scientists' ability to manage ecosystems, conserve species, and predict the consequences of environmental change. That knowledge can be equally powerful at the microbial scale and is likely to also have fruitful application beyond ecology in industry and in medicine. Accordingly, the growth and mortality rates revealed by qSIP provide powerful new measures of how microorganisms interact in complex ecosystems.

## ACKNOWLEDGMENTS

This work was supported in part by the National Science Foundation (DEB-1241094, DEB-1146449), the Department of Energy's Biological Systems Science Division, Program in Genomic Science (DE-SC0016207), and the Technology Research Initiative Fund from the State of Arizona. Work at Lawrence Livermore National Laboratory (LLNL) was funded by the Department of Energy through the Genome Sciences Program under contracts SCW1024 and SCW1590 and performed under the auspices of LLNL under Contract DE-AC52-07NA27344. Comments from J. Cliff and two anonymous reviewers improved the manuscript.

## LITERATURE CITED

- Acinas, S. G., L. A. Marcelino, V. Klepac-Ceraj, and M. F. Polz. 2004. Divergence and redundancy of 16S rRNA sequences in genomes with multiple *rnn* operons. *Journal of Bacteriology* 186:2629–2635.
- Allison, S. D., and P. M. Vitousek. 2004. Rapid nutrient cycling in leaf litter from invasive plants in Hawai'i. *Oecologia* 141:612–619.
- Aronesty, E. 2011. ea-utils: command-line tools for processing biological sequencing data. <https://github.com/ExpressionAnalysis/ea-utils>
- Bååth, E. 1990. Thymidine incorporation into soil bacteria. *Soil Biology and Biochemistry* 22:803–810.
- Bååth, E. 1992. Thymidine incorporation into macromolecules of bacteria extracted from soil by homogenization-centrifugation. *Soil Biology and Biochemistry* 24:1157–1165.
- Bååth, E. 1994a. Measurement of protein synthesis by soil bacterial assemblages with the leucine incorporation technique. *Biology and Fertility of Soils* 17:147–153.
- Bååth, E. 1994b. Thymidine and leucine incorporation in soil bacteria with different cell size. *Microbial Ecology* 27:267–278.
- Bååth, E. 1998. Growth rates of bacterial communities in soils at varying pH: a comparison of the thymidine and leucine incorporation techniques. *Microbial Ecology* 36:316–327.
- Bates, S. T., D. Berg-Lyons, J. G. Caporaso, W. A. Walters, R. Knight, and N. Fierer. 2011. Examining the global distribution of dominant archaeal populations in soil. *ISME Journal* 5:908–917.
- Berry, D., K. B. Mahfoudh, M. Wagner, and A. Loy. 2011. Barcoded primers used in multiplex amplicon pyrosequencing bias amplification. *Applied and Environmental Microbiology* 77:7846–7849.
- Berry, D., and S. Widder. 2014. Deciphering microbial interactions and detecting keystone species with co-occurrence networks. *Frontiers in Microbiology* 5:art219.
- Blankinship, J. C., J. R. Brown, P. Dijkstra, M. C. Allwright, and B. A. Hungate. 2010. Response of terrestrial  $\text{CH}_4$  uptake to interactive changes in precipitation and temperature along a climatic gradient. *Ecosystems* 13:1157–1170.
- Blazewicz, S. J., E. Schwartz, and M. K. Firestone. 2014. Growth and death of bacteria and fungi underlie rainfall-induced carbon dioxide pulses from seasonally dried soil. *Ecology* 95:1162–1172.
- Bloem, J., P. C. de Ruyter, G. J. Koopman, G. Lebbink, and L. Brussaard. 1992. Microbial numbers and activity in dried and rewetted arable soil under integrated and conventional management. *Soil Biology and Biochemistry* 24:655–665.
- Bokulich, N. A., S. Subramanian, J. J. Faith, D. Gevers, J. I. Gordon, R. Knight, D. A. Mills, and J. G. Caporaso. 2013. Quality-filtering vastly improves diversity estimates from Illumina amplicon sequencing. *Nature Methods* 10:57–59.
- Bölter, M., J. Bloem, K. Meiners, and R. Möller. 2002. Enumeration and biovolume determination of microbial cells – a methodological review and recommendations for applications in ecological research. *Biology and Fertility of Soils* 36:249–259.
- Brown, C. T., M. R. Olm, B. C. Thomas, and J. F. Banfield. 2016. Measurement of bacterial replication rates in microbial communities. *Nature Biotechnology* 34:1256–1263.
- Caporaso, J. G., K. Bittinger, F. D. Bushman, T. Z. DeSantis, G. L. Andersen, and R. Knight. 2010a. PyNAST: a flexible tool for aligning sequences to a template alignment. *Bioinformatics* 26:266–267.
- Caporaso, J. G., et al. 2010b. QIIME allows analysis of high-throughput community sequencing data. *Nature Methods* 7:335–336.

- Caporaso, J. G., C. L. Lauber, W. A. Walters, D. Berg-  
Lyons, C. A. Lozupone, P. J. Turnbaugh, N. Fierer,  
and R. Knight. 2011. Global patterns of 16S rRNA  
diversity at a depth of millions of sequences per  
sample. *Proceedings of the National Academy of  
Sciences USA* 108:4516–4522.
- Caporaso, J. G., et al. 2012. Ultra-high-throughput  
microbial community analysis on the Illumina  
HiSeq and MiSeq platforms. *ISME Journal* 6:1621–  
1624.
- Caraco, N. F., J. J. Cole, P. A. Raymond, D. L. Strayer,  
M. L. Pace, S. E. G. Findlay, and D. T. Fischer. 1997.  
Zebra mussel invasion in a large, turbid river: phy-  
toplankton response to increased grazing. *Ecology*  
78:588–602.
- Carpenter, S. R., J. F. Kitchell, J. R. Hodgson, P. A.  
Cochran, J. J. Elser, M. M. Elser, D. M. Lodge,  
D. Kretchmer, X. He, and C. N. von Ende. 1987.  
Regulation of lake primary productivity by food  
web structure. *Ecology* 68:1863–1876.
- Case, R. J., Y. Boucher, I. Dahllorf, C. Holmstrom, W. F.  
Doolittle, and S. Kjelleberg. 2007. Use of 16S rRNA  
and *rpoB* genes as molecular markers for microbial  
ecology studies. *Applied and Environmental  
Microbiology* 73:278–288.
- Chapin, F. S., L. R. Walker, C. L. Fastie, and L. C.  
Sharman. 1994. Mechanisms of primary succession  
following deglaciation at Glacier Bay, Alaska.  
*Ecological Monographs* 64:149–175.
- Cheng, W. 2009. Rhizosphere priming effect: its func-  
tional relationships with microbial turnover, evap-  
otranspiration, and C–N budgets. *Soil Biology and  
Biochemistry* 41:1795–1801.
- Chu, H., N. Fierer, C. L. Lauber, J. G. Caporaso, R.  
Knight, and P. Grogan. 2010. Soil bacterial diversity  
in the Arctic is not fundamentally different from  
that found in other biomes. *Environmental Micro-  
biology* 12:2998–3006.
- Connell, J. H. 1978. Diversity in tropical rain forests  
and coral reefs. *Science* 199:1302–1310.
- Connell, J. H., and R. O. Slatyer. 1977. Mechanisms of  
succession in natural communities and their role in  
community stability and organization. *American  
Naturalist* 111:1119–1144.
- Coyotzi, S., J. Pratscher, J. C. Murrell, and J. D.  
Neufeld. 2016. Targeted metagenomics of active  
microbial populations with stable-isotope probing.  
*Current Opinion in Biotechnology* 41:1–8.
- Crosby, L. D., and C. S. Criddle. 2003. Understanding  
bias in microbial community analysis techniques  
due to *rnm* operon copy number heterogeneity.  
*BioTechniques* 34:790–802.
- DeSantis, T. Z., P. Hugenholtz, N. Larsen, M. Rojas, E. L.  
Brodie, K. Keller, T. Huber, D. Dalevi, P. Hu, and G.  
L. Andersen. 2006. Greengenes, a chimera-checked  
16S rRNA gene database and workbench compati-  
ble with ARB. *Applied and Environmental Micro-  
biology* 72:5069–5072.
- Dhanasekaran, S., T. M. Doherty, J. Kenneth, and TB  
Trials Study Group. 2010. Comparison of different  
standards for real-time PCR-based absolute quan-  
tification. *Journal of Immunological Methods*  
354:34–39.
- Ducklow, H. W., M.-L. Dickson, D. L. Kirchman, G.  
Steward, J. Orchardo, J. Marra, and F. Azam. 2000.  
Constraining bacterial production, conversion effi-  
ciency and respiration in the Ross Sea, Antarctica,  
January–February, 1997. *Deep Sea Research Part II:  
Topical Studies in Oceanography* 47:3227–3247.
- Edgar, R. C. 2010. Search and clustering orders of  
magnitude faster than BLAST. *Bioinformatics* 26:  
2460–2461.
- Ellison, A. M., et al. 2005. Loss of foundation species:  
consequences for the structure and dynamics of  
forested ecosystems. *Frontiers in Ecology and the  
Environment* 3:479–486.
- Elser, J. J., D. R. Dobberfuhl, N. A. MacKay, and J. H.  
Schampel. 1996. Organism size, life history, and  
N:P stoichiometry. *BioScience* 46:674–684.
- Franzluebbers, A. J. 1999. Potential C and N mineral-  
ization and microbial biomass from intact and  
increasingly disturbed soils of varying texture. *Soil  
Biology and Biochemistry* 31:1083–1090.
- Grace, J. B. 1951. The life cycle of *Sporocytophaga*.  
*Microbiology* 5:519–524.
- Harris, D., and E. A. Paul. 1994. Measurement of bacte-  
rial growth rates in soil. *Applied Soil Ecology*  
1:277–290.
- Harris, J. K., et al. 2013. Phylogenetic stratigraphy in  
the Guerrero Negro hypersaline microbial mat.  
*ISME journal* 7:50–60.
- Hayer, M., E. Schwartz, J. C. Marks, B. J. Koch, E. M.  
Morrissey, A. A. Schuettenberg, and B. A. Hungate.  
2016. Identification of growing bacteria during  
litter decomposition in freshwater through H<sub>2</sub><sup>18</sup>O  
quantitative stable isotope probing: growing  
bacteria during litter decomposition in freshwater.  
*Environmental Microbiology Reports* 8:975–982.
- Huffaker, C. B. 1958. Experimental studies on preda-  
tion: dispersion factors and predator–prey oscilla-  
tions. *Hilgardia* 27:343–383.
- Hungate, B. A., et al. 2015. Quantitative microbial  
ecology through stable isotope probing. *Applied  
and Environmental Microbiology* 81:7570–7581.
- Hunt, H. W., D. C. Coleman, E. R. Ingham, R. E.  
Ingham, E. T. Elliott, J. C. Moore, S. L. Rose, C. P. P.  
Reid, and C. R. Morley. 1987. The detrital food web  
in a shortgrass prairie. *Biology and Fertility of Soils*  
3:57–68.
- Hutchinson, G. E. 1942. Addendum. *Ecology* 23:417–418.

- Kanagawa, T. 2003. Bias and artifacts in multitemplate polymerase chain reactions (PCR). *Journal of Bioscience and Bioengineering* 96:317–323.
- Korem, T., et al. 2015. Growth dynamics of gut microbiota in health and disease inferred from single metagenomic samples. *Science* 349:1101–1106.
- Kouno, K., J. Wu, and P. C. Brookes. 2002. Turnover of biomass C and P in soil following incorporation of glucose or ryegrass. *Soil Biology and Biochemistry* 34:617–622.
- Kozarewa, I., Z. Ning, M. A. Quail, M. J. Sanders, M. Berriman, and D. J. Turner. 2009. Amplification-free Illumina sequencing-library preparation facilitates improved mapping and assembly of (G+C)-biased genomes. *Nature Methods* 6:291–295.
- Langille, M. G. I., et al. 2013. Predictive functional profiling of microbial communities using 16S rRNA marker gene sequences. *Nature Biotechnology* 31: 814–821.
- Lazcano, A. 2011. Natural history, microbes and sequences: Shouldn't we look back again to organisms? *PLoS ONE* 6:e21334.
- Lindeman, R. L. 1942. The trophic-dynamic aspect of ecology. *Ecology* 23:399–417.
- Lovett, G. M., C. D. Canham, M. A. Arthur, K. C. Weathers, and R. D. Fitzhugh. 2006. Forest ecosystem responses to exotic pests and pathogens in eastern North America. *BioScience* 56:395–405.
- Maestre, F. T., et al. 2015. Increasing aridity reduces soil microbial diversity and abundance in global drylands. *Proceedings of the National Academy of Sciences USA* 112:15684–15689.
- Markowitz, V. M., et al. 2012. IMG: the integrated microbial genomes database and comparative analysis system. *Nucleic Acids Research* 40:D115–D122.
- Martin-Laurent, F., L. Philippot, S. Hallet, R. Chaussod, J. C. Germon, G. Soulas, and G. Catroux. 2001. DNA extraction from soils: old bias for new microbial diversity analysis methods. *Applied and Environmental Microbiology* 67:2354–2359.
- McHugh, T. A., G. W. Koch, and E. Schwartz. 2014. Minor changes in soil bacterial and fungal community composition occur in response to monsoon precipitation in a semiarid grassland. *Microbial Ecology* 68:370–378.
- Morris, W. F., and D. F. Doak. 2002. *Quantitative conservation biology: theory and practice of population viability analysis*. Sinauer Associates, Sunderland, Massachusetts, USA.
- Morrissey, E. M., R. L. Mau, E. Schwartz, T. A. McHugh, P. Dijkstra, B. J. Koch, J. C. Marks, and B. A. Hungate. 2017. Bacterial carbon use plasticity, phylogenetic diversity and the priming of soil organic matter. *ISME Journal* 11:1890–1899.
- Morrissey, E. M., et al. 2016. Phylogenetic organization of bacterial activity. *ISME Journal* 10:2336–2340.
- Moyle, P. B., and T. Light. 1996. Biological invasions of fresh water: empirical rules and assembly theory. *Biological Conservation* 78:149–161.
- Newell, S. Y., and R. D. Fallon. 1991. Toward a method for measuring instantaneous fungal growth rates in field samples. *Ecology* 72:1547–1559.
- Odum, E. P. 1960. Organic production and turnover in old field succession. *Ecology* 41:34–49.
- Paine, R. T. 1966. Food web complexity and species diversity. *American Naturalist* 100:65–75.
- Perele, L. W., and J. C. Munch. 2005. Microbial immobilisation and turnover of <sup>13</sup>C labelled substrates in two arable soils under field and laboratory conditions. *Soil Biology and Biochemistry* 37:2263–2272.
- Pham, V. H. T., and J. Kim. 2012. Cultivation of unculturable soil bacteria. *Trends in Biotechnology* 30: 475–484.
- Post, W. M., and S. L. Pimm. 1983. Community assembly and food web stability. *Mathematical Biosciences* 64:169–192.
- Power, M. E., D. Tilman, J. A. Estes, B. A. Menge, W. J. Bond, L. S. Mills, G. Daily, J. C. Castilla, J. Lubchenco, and R. T. Paine. 1996. Challenges in the quest for keystones. *BioScience* 46:609–620.
- Prosser, J. I., et al. 2007. The role of ecological theory in microbial ecology. *Nature Reviews Microbiology* 5:384–392.
- R Core Team. 2015. *R: a language and environment for statistical computing*. R Foundation for Statistical Computing, Vienna, Austria.
- Radajewski, S., P. Ineson, N. R. Parekh, and J. C. Murrell. 2000. Stable-isotope probing as a tool in microbial ecology. *Nature* 403:646–649.
- Reichenbach, H. 2006. The order Cytophagales. Pages 549–590 in M. Dworkin, S. Falkow, E. Rosenberg, K.-H. Schleifer, and E. Stackebrandt, editors. *The prokaryotes*. Springer, New York, New York, USA.
- Rohland, N., and D. Reich. 2012. Cost-effective, high-throughput DNA sequencing libraries for multiplexed target capture. *Genome Research* 22:939–946.
- Rousk, J., and E. Bååth. 2011. Growth of saprotrophic fungi and bacteria in soil. *FEMS Microbiology Ecology* 78:17–30.
- Schmid-Araya, J. M., A. G. Hildrew, A. Robertson, P. E. Schmid, and J. Winterbottom. 2002. The importance of meiofauna in food webs: evidence from an acid stream. *Ecology* 83:1271–1285.
- Schwartz, E. 2007. Characterization of growing microorganisms in soil by stable isotope probing with H<sub>2</sub><sup>18</sup>O. *Applied and Environmental Microbiology* 73:2541–2546.
- Schwartz, E., M. Hayer, B. A. Hungate, B. J. Koch, T. A. McHugh, W. Mercurio, E. M. Morrissey, and



- K. Soldanova. 2016. Stable isotope probing with  $^{18}\text{O}$ -water to investigate microbial growth and death in environmental samples. *Current Opinion in Biotechnology* 41:14–18.
- Spohn, M., K. Klaus, W. Wanek, and A. Richter. 2016. Microbial carbon use efficiency and biomass turnover times depending on soil depth – implications for carbon cycling. *Soil Biology and Biochemistry* 96:74–81.
- Stewart, E. J. 2012. Growing unculturable bacteria. *Journal of Bacteriology* 194:4151–4160.
- Strayer, D. L., N. F. Caraco, J. J. Cole, S. Findlay, and M. L. Pace. 1999. Transformation of freshwater ecosystems by bivalves. *BioScience* 49:19–27.
- Tedersoo, L., R. H. Nilsson, K. Abarenkov, T. Jairus, A. Sadam, I. Saar, M. Bahram, E. Bechem, G. Chuyong, and U. Kõljalg. 2010. 454 Pyrosequencing and Sanger sequencing of tropical mycorrhizal fungi provide similar results but reveal substantial methodological biases. *New Phytologist* 188:291–301.
- Tewksbury, J. J., et al. 2014. Natural history's place in science and society. *BioScience* 64:300–310.
- Tibbles, B. J., and J. M. Harris. 1996. Use of radiolabelled thymidine and leucine to estimate bacterial production in soils from continental Antarctica. *Applied and Environmental Microbiology* 62:694–701.
- Tilman, D. 1977. Resource competition between planktonic algae: an experimental and theoretical approach. *Ecology* 58:338–348.
- Tilman, D. 1985. The resource-ratio hypothesis of plant succession. *American Naturalist* 125:827–852.
- Tilman, D. 1999. The ecological consequences of changes in biodiversity: a search for general principles. *Ecology* 80:1455–1474.
- Uhlířová, E., and H. Šantrůčková. 2003. Growth rate of bacteria is affected by soil texture and extraction procedure. *Soil Biology and Biochemistry* 35: 217–224.
- Vitousek, P. M., and L. R. Walker. 1989. Biological invasion by *Myrica faya* in Hawai'i: plant demography, nitrogen fixation, ecosystem effects. *Ecological Monographs* 59:247–265.
- Wang, Q., G. M. Garrity, J. M. Tiedje, and J. R. Cole. 2007. Naïve Bayesian classifier for rapid assignment of rRNA sequences into the new bacterial taxonomy. *Applied and Environmental Microbiology* 73:5261–5267.
- Weyers, H. S., and K. Suberkropp. 1996. Fungal and bacterial production during the breakdown of yellow poplar leaves in 2 streams. *Journal of the North American Benthological Society* 15: 408–420.